WARSAW UNIVERSITY OF TECHNOLOGY Index 351733
FACULTY OF CIVIL ENGINEERING
COMMITTEE FOR CIVIL AND WATER ENGINEERING
POLISH ACADEMY OF SCIENCES ISSN 1230-2945

DOI: 10.24425/ace.2026.1331

ARCHIVES OF CIVIL ENGINEERING

Vol. LXXII ISSUE 3 2026

pp. 23–33

Research paper

Bleeding and rheological properties of alkali activated fly ash-slag at different temperatures

Shaoju Hao[1], Xiaoxu Chen[2]

Abstract: The bleeding and rheological properties of three sets of alkali-activated fly ash-slag pastes at different temperatures were investigated. The results indicate that the ratio of slag-to-fly ash and temperature have a significant impact on the bleeding rate and rheological properties of the paste. The bleeding rate of alkali-activated fly ash-slag system gradually decreases with the increase of temperature. And as the content of fly ash gradually increases, the bleeding rate further increases. In addition, the thixotropic area of the paste exhibits a change similar to the yield stress, that is, when the temperature and fly ash content increase, both rheological parameters significantly increase. In the early stage of hydration, the degree of hydration of all samples is not high, manifested as no significant dissolution of fly ash and slag particles observed. At the same degree of bleeding, the paste with higher temperature exhibit relatively higher yield stress and lower thixotropy, indicating that the accelerated hydration rate of pastes in high-temperature environments leads to more stable microstructures.

Keywords: alkali-activated materials, fly ash, slag, rheological properties, bleeding rate

[1]MSc., Eng., Henan Radio & Television University, Zhengzhou, 450046, China, e-mail: haoshaoju@haou.edu.cn, ORCID: 0009-0001-9542-6551
[2]MSc., Eng., Henan Open University, Zhengzhou 450045, China, e-mail: maychendaxu@163.com, ORCID: 0009-0000-4925-5029

1. Introduction

The civil engineering industry has developed rapidly in recent decades, and the widespread use of concrete materials has inevitably led to an increasing demand for cement. However, the calcination of traditional Portland cement (PC) clinker emits a large amount of carbon dioxide and consumes fossil energy, making it an important source of carbon emissions in the construction industry [1–3]. Using some industrial waste materials to partially or completely replace Portland cement is an important measure to alleviate cement related carbon emissions [4, 5]. Fly ash (FA), granulated blast furnace slag powder, and silica fume are some typical industrial wastes [6, 7]. Their addition can cause pozzolanic reaction in the system, providing reasonable strength for the structure.

In addition to incorporating mineral admixtures such as fly ash into Portland cement to form a composite cementitious system, alkali activated cementitious materials (geopolymer materials) are increasingly receiving attention from many scholars due to their characteristic of not requiring cement at all [8–10]. Therefore, it can also be referred to as a substitute cementitious material for the Portland cement system. Compared with the Portland cement system, the reaction mechanism of alkali activated materials is different, mainly depending on the composition of the aluminosilicate used. Therefore, the reaction mechanism of alkaline activated system can be mainly divided into high calcium and low calcium alkaline activation [11]. In high calcium cementitious materials, the main material used as a cementitious material is calcium aluminum silicate. Its reaction can form a dense cement matrix and exhibit good mechanical properties. However, low calcium systems mainly rely on the polymerization of aluminosilicates to achieve densification of the microstructure of cementitious materials [12]. Whether in high calcium or low calcium systems, the performance of alkali activated cementitious materials is mainly determined by the characteristics of hydration products, namely calcium aluminosilicate (C–A–S–H) and sodium aluminosilicate (N–A–S–H), their distribution in the matrix, as well as the morphology and density of the overlap [13, 14].

Although many scholars have conducted extensive research on the later mechanical properties and durability of alkali activated materials, further exploration is still needed for their early performance, namely the rheological properties in the fresh state. Reasonable workability parameters can make it easy for alkali activated materials to achieve dense filling in the template space during construction, thereby improving construction efficiency [15]. The workability measured during construction corresponds to the rheological properties of the paste or concrete system [16, 17]. Palacios et al. [18] believe that the rheological properties of alkali activated materials are influenced by the type and dosage of the activator. The paste using sodium hydroxide or sodium carbonate as activators typically exhibits properties of the Bingham model, where shear stress and rate exhibit an approximately linear relationship. In addition, Albar et al. [19] believe that the improved Bingham model, which introduces a quadratic term to characterize the nonlinear relationship on the original model, can effectively calculate the rheological parameters of the fly ash-granulated blast furnace slag (GBFS) binary system excited by sodium silicate and sodium hydroxide. Polycarboxylic acid based high-efficiency water reducing agents have also been proven to improve the flowability of alkali activated materials, which mainly depends on the properties of the alkali activated agent [20].

In addition to the mixing ratio factors of the cementitious material itself, environmental temperature and bleeding can also have a significant impact on the rheological properties of the material. Cement paste may exhibit bleeding characteristics under the influence of gravity and physical and chemical reactions. When the bleeding rate is too high, the particles in the cement suspension will precipitate, and the moisture will move up, thereby affecting the uniformity and rheology of the paste. Based on the above background, this study aims to investigate the influence of different mix proportions and temperatures on the rheological properties and bleeding characteristics of alkali activated fly ash-slag paste. A rheometer was used to systematically test the rheological properties of the paste, and at the same time, the bleeding characteristics of the paste were characterized, providing important experimental evidence for the changes in the rheological properties of alkali activated fly ash-slag at different temperatures.

2. Experiments

2.1. Materials and mix proportions

Fly ash is provided by Shijiazhuang Beno Mineral Products Co., Ltd. and is classified as Class F, Grade I. The slag is provided by Jintai Cheng Technology Group Co., Ltd. and is classified as S95 grade. Table 1 shows the chemical composition of fly ash and slag. Select NaOH with a purity of up to 99% as the alkaline activator.

To avoid the impact of the exothermic process on the paste, NaOH was dissolved in water and placed in a container for 24 hours to allow it to return to room temperature. Then mix the NaOH solution thoroughly with the powder.

Table 1. Chemical compositions of fly ash ans slag (%)

	SiO_2	Al_2O_3	CaO	Fe_2O_3	MgO	SO_3	Na_2O
FA	51.72	30.85	5.09	5.59	0.61	0.58	0.51
Slag	31.33	14.71	41.09	1.15	5.88	2.21	0.39

The combinations used in this study are shown in Table 2, where the mass ratios of fly ash and slag are 3:7, 5:5, and 7:3, respectively. On this basis, 4% sodium hydroxide was added as an activator. Weigh fly ash, slag, and NaOH solution separately according to the mass ratio. Use an electric stirrer to stir at a speed of 300 rpm for 5 minutes. In order to minimize the influence of temperature, the stirring process is carried out in a constant temperature water bath at the corresponding temperature. When stirring, seal the top of the container with plastic wrap to reduce water evaporation.

Table 2. Mix proportions of alkali-activated fly ash-slag

Sample	FA (%)	Slag (%)	w/b	Alkaline activator (%)
1	30	70	0.6	4
2	50	50	0.6	4
3	70	30	0.6	4

2.2. Methodology

2.2.1. Bleeding tests

Use the static method shown in Figure 1 to test the degree of bleeding of cement paste. At 20°C, 40°C, testing the degree of bleeding of three groups of samples at 60°C and 80°C. After preparing the slurry at various temperatures, pour it into a 100 mL volumetric flask. The measuring cylinder is sealed with cling film. The bleeding test is conducted in a constant temperature and humidity curing box. During the test, the liquid level height of the slurry is recorded every 10 minutes for 120 minutes. The highest bleeding rate during the test period is taken as the bleeding rate at that temperature and mix ratio. Prepare 3 sets of samples for each mix proportion to ensure the reliability of the test data, and take the average of the three results.

The bleeding rate of the slurry refers to the ratio of the amount of water secreted to the volume of the original slurry. Therefore, the formula for calculating the bleeding rate is as follows:

$$\eta = \frac{V_w}{V_0} \times 100\% \tag{2.1}$$

Among them, η is the bleeding rate of cement paste, V_w is the volume of bleeding in the cement paste, and V_0 refers to the initial volume of the cement paste (100 mL).

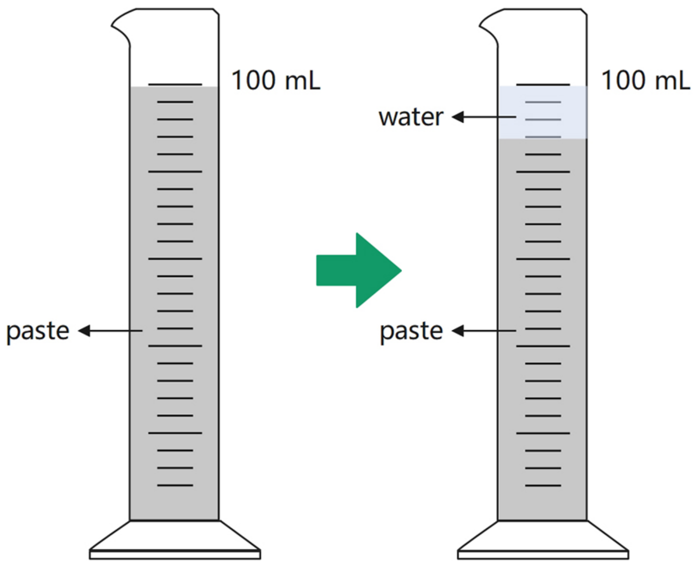

Fig. 1. Bleeding test procedure

2.2.2. Rheology tests

The MCR 102e rheometer from Anton Paar company was used to conduct rheological tests on the mix proportion slurry in this study. The testing system adopted is shown in Figure 2. In order to ensure consistent shear of the slurry before testing to counteract the potential impact of mixing time on the rheological properties of the slurry, a pre shear rate of 100 s^{-1} was applied to each group of slurry for 30 seconds. Subsequently, the shear rate increases in the pattern of rising steps in Figure 2 and decreases in the same way. Record the shear stress at each step rate in the descending section and use it as the stress value at that rate.

The improved Bingham model is used to characterize the yield stress of the slurry, and its calculation formula is:

$$\tau = \tau_0 + \mu\gamma + c\gamma^2 \tag{2.2}$$

Among them, τ is the shear stress (Pa), τ_0 is the yield stress (Pa), μ is the viscosity (Pa·s), γ is the shear rate (s^{-1}), and c is the quadratic coefficient. In addition to calculating the yield stress, the thixotropy of the mixture can also be obtained by the area enclosed by the up and down curves of the rheological curve of the slurry, that is, the area of the thixotropic hysteresis loop.

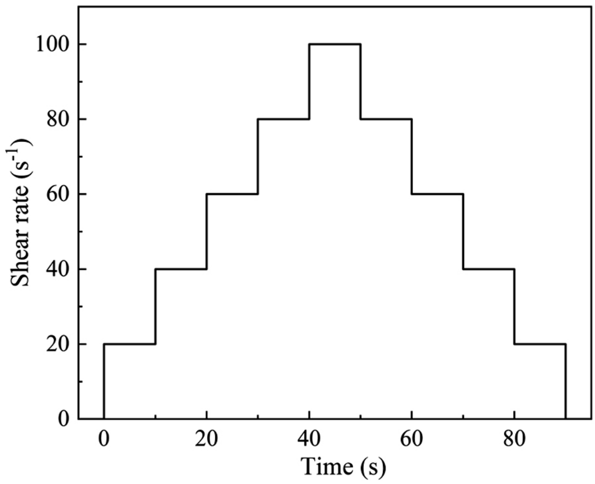

Fig. 2. Rheological test system of this study

3. Results

3.1. Bleeding rate

The variation of bleeding rate of alkali activated fly ash-slag composite cementitious system with temperature under different mix ratios is shown in Figure 3. From Figure 3, it can be seen that as the temperature increases, the bleeding rate of each group of slurry gradually decreases, and their relationship is approximately linear. The amount of bleeding in all slurries increases rapidly in the early stages of hydration, and gradually stabilizes after reaching the final bleeding rate. Therefore, the final bleeding rate within the test section is the stable bleeding rate. Comparing the bleeding rates of three different mix proportions of slurry, it can be found that sample 3 with a higher content of fly ash exhibits the highest bleeding rate, indicating that the addition of fly ash exacerbates the bleeding behavior of the slurry.

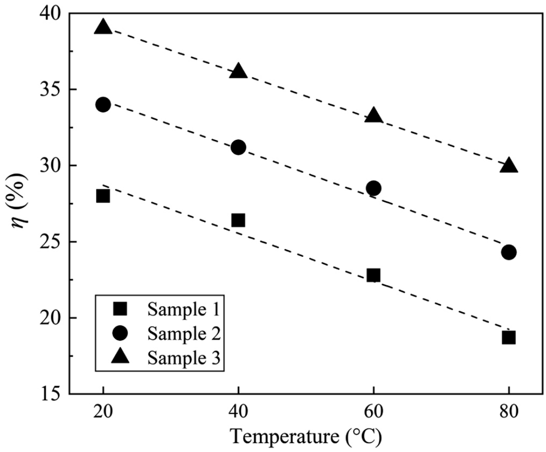

Fig. 3. Bleeding rate of alkali-activated fly ash-slag system

3.2. Rheology

Figure 4 shows the flow curve of alkali activated fly ash-slag at 20°C. It can be observed that the yield stress corresponding to the upward curve obtained by the testing method in Figure 2 is greater than that of the downward curve. By fitting the downward flow curve in Figure 4, the fitting data in Table 3 and the yield stress in Figure 5 can be obtained. It can be observed that sample 1 has the highest yield stress at different temperatures. After the temperature increased from 20°C to 40°C, the yield stress of samples 1 and 2 decreased slightly. However, as the temperature continues to rise, the yield stress of the three groups of alkali activated fly ash-slag shows an upward trend and reaches its peak at 80°C. The yield stresses of the three slurries at 80°C are 78.4 Pa, 71.4 Pa, and 57.8 Pa, respectively.

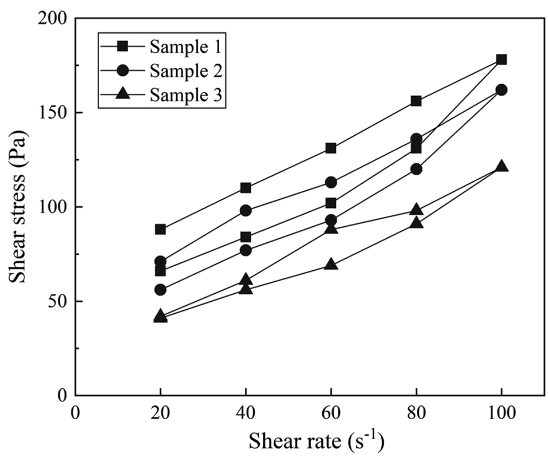

Fig. 4. Flow curves of alkali-activated fly ash-slag at 20°C

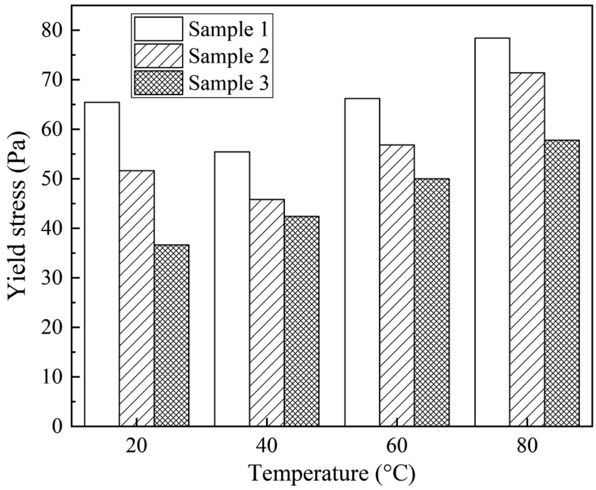

Fig. 5. Yield stress of alkali-activated fly ash-slag at 20°C

Table 3. Fitting equation based on the modified Bingham model

Sample	Mass ratio		Temperature	Modified Bingham model	R^2
	FA	Slag			
1	30	70	20	$\tau = 65.4 + 0.123\gamma + 0.012\gamma 2$	0.9915
2	50	50	20	$\tau = 51.6 + 0.139\gamma + 0.009\gamma 2$	0.9875
3	70	30	20	$\tau = 36.6 + 0.139\gamma + 0.006\gamma 2$	0.9938
4	30	70	40	$\tau = 55.4 + 0.271\gamma + 0.011\gamma 2$	0.9803
5	50	50	40	$\tau = 45.8 + 0.5\gamma + 0.007\gamma 2$	0.9928
6	70	30	40	$\tau = 42.4 + 0.136\gamma + 0.009\gamma 2$	0.9922
7	30	70	60	$\tau = 66.2 + 0.256\gamma + 0.012\gamma 2$	0.9997
8	50	50	60	$\tau = 56.8 + 0.161\gamma + 0.011\gamma 2$	0.9952
9	70	30	60	$\tau = 50 + 0.387\gamma + 0.008\gamma 2$	0.9898
10	30	70	80	$\tau = 78.4 + 0.206\gamma + 0.012\gamma 2$	0.9842
11	50	50	80	$\tau = 71.4 + 0.189\gamma + 0.012\gamma 2$	0.9959
12	70	30	80	$\tau = 57.8 + 0.295\gamma + 0.011\gamma 2$	0.9966

3.3. Thixotropy

The area enclosed by the upward and downward flow curves can be used to calculate the thixotropic ring area of the slurry. Generally speaking, the larger the area, the greater the decrease in viscosity of the slurry under shear force, corresponding to higher thixotropy.

Figure 6 shows the thixotropic area of three groups of slurries at different temperatures. It can be observed that the change in thixotropic area is similar to the yield stress, but the thixotropic area shows a trend of increasing with temperature, that is, it does not decrease at 40°C like the yield stress. In addition, sample 1 exhibited significantly greater thixotropy than the other mix proportions, indicating that alkali activated systems with higher slag content have greater thixotropy. This may be because the surface of slag particles is more irregular compared to fly ash particles, requiring greater shear force to promote the flow of the slurry. On the contrary, fly ash, due to its circular shape, can promote easier flow of the slurry.

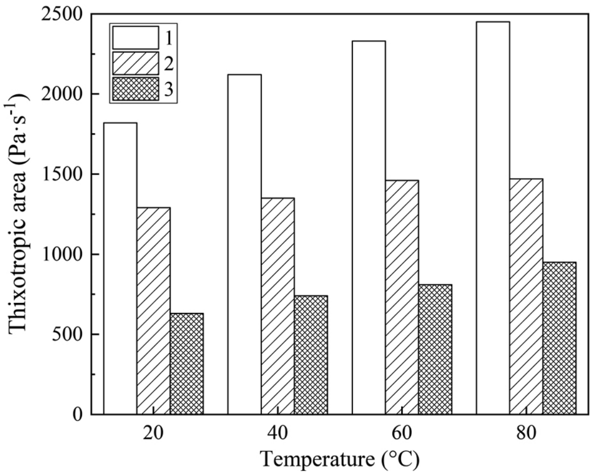

Fig. 6. Thixotropic area of alkali-activated fly ash-slag at 20°C

4. Discussion

Figure 7 shows the variation trend of yield stress with water bleeding rate for three groups of alkali excited samples at different temperatures, and the corresponding equations were obtained using the fitting function method. When the temperature is within the range of 20–80°C, the linear model can fit the relationship between them well. From the calculation results in Figure 8, it can be seen that as the bleeding rate increases, the yield stress of the slurry decreases. During the mixing process of cement and water, cement particles will disperse into the aqueous suspension. Water in suspension can be divided into three categories based on its different forms of existence: water that fills the gaps between solid particles, water that is encapsulated by flocculation structures, and free water that forms a water film on the surface of particles [21]. However, under the self gravity of cement clinker particles, the particles will sink after a period of standing, while the moisture will move up. This bleeding phenomenon will reduce the initial network structure formed by the original suspension, thereby reducing the yield stress of the slurry. In addition, the results in Figure 8 also indicate that the increase in temperature not only reduces the degree of bleeding of the slurry, but also increases the yield stress of the slurry, which is due to the acceleration of cement hydration caused by the increase in temperature.

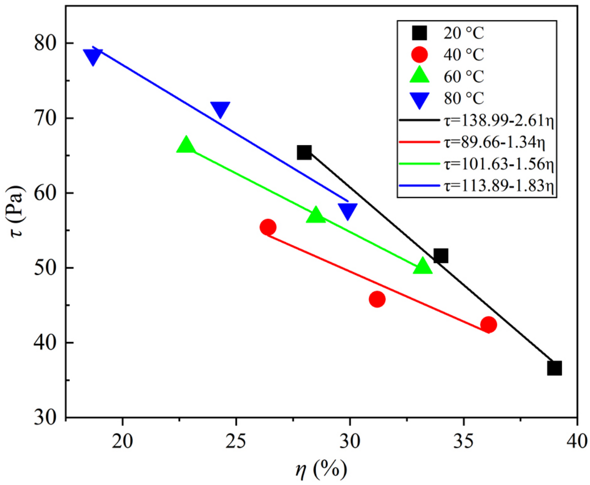

Fig. 7. Relationship between yield stress and bleeding rate

Figure 8 shows the relationship between the area of the thixotropic ring and the bleeding rate of cement slurry. It can be observed that the change in thixotropy is very similar to the yield stress, that is, both decrease linearly with the increase of slurry bleeding rate. At the same degree of bleeding, the slurry with higher temperature exhibits relatively lower thixotropy, indicating that the accelerated hydration rate of the slurry under high temperature environment leads to a more stable slurry structure. The increase in temperature can not only increase the yield stress of alkali activated fly ash-slag slurry, reduce the thixotropy of the system, but also decrease the bleeding rate.

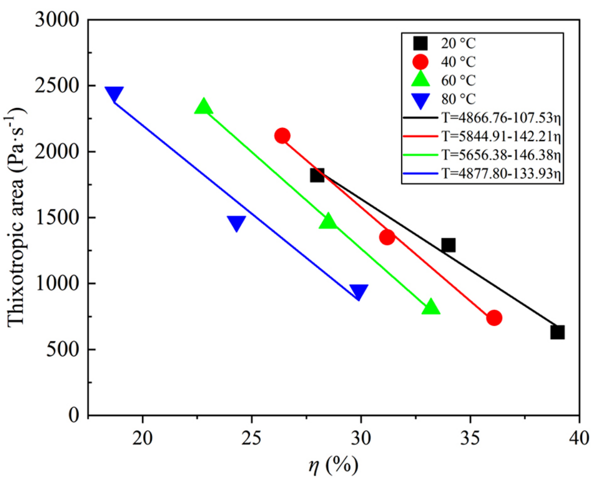

Fig. 8. Relationship between thixotropic area and bleeding rate

5. Conclusions

The bleeding and rheological properties of three sets of alkali-activated fly ash-slag pastes at different temperatures were investigated in detail. Based on the experimental analysis, the following conclusions can be drawn:

(1) For the three mix proportions studied in this study, the bleeding rate of the alkali activated fly ash-slag system gradually decreases with increasing temperature. And as the amount of fly ash gradually increases, the bleeding rate further increases.

(2) The shear stress corresponding to the upward curve of each group of slurry is greater than that of the downward curve. The yield stress based on the downward curve gradually decreases with the increase of fly ash content, and when the temperature is greater than 40°C, the yield stress gradually increases with the increase of temperature.

(3) The change trend of the thixotropic area of the slurry is similar to the yield stress, that is, when the temperature increases or the fly ash content decreases, the thixotropic area significantly increases. In the early stage of hydration, the hydration degree of the samples was not high, manifested as no significant dissolution of fly ash and slag particles observed.

References

[1] C. Shi, A.F. Jiménez, and A. Palomo, "New cements for the 21st century: The pursuit of an alternative to Portland cement", *Cement and Concrete Research*, vol. 41, no. 7, pp. 750–763, 2011, doi: 10.1016/j.cemconres.2011.03.016.

[2] S. Tamta, R. Chaudhury, U. Sharma, P.C. Thapliyal, and L.P. Singh, "Low-CO2 emission strategies to achieve net zero target in cement sector", *Journal of Cleaner Production*, vol. 417, art. no. 137466, 2023, doi: 10.1016/j.jclepro.2023.137466.

[3] Y. Guo, et al., "A review of low-carbon technologies and projects for the global cement industry", *Journal of Environmental Sciences*, vol. 136, pp. 682–697, 2024, doi: 10.1016/j.jes.2023.01.021.

[4] T. Ray, N.R. Mohanta, M.H. Kumar, I.S. Macharyulu, and S. Samantaray, "Study of effect of temperature on behavior of alkali activated slag concrete", *Materials Today: Proceedings*, vol. 43, Part 2, pp. 1352–1357, 2021, doi: 10.1016/j.matpr.2020.09.169.

[5] R. Snellings, P. Suraneni, and J. Skibsted, "Future and emerging supplementary cementitious materials", *Cement and Concrete Research*, vol. 171, art. no. 107199, 2023, doi: 10.1016/j.cemconres.2023.107199.

[6] B. Lothenbach, K. Scrivener, and R.D. Hooton, "Supplementary cementitious materials", *Cement and Concrete Research*, vol. 41, no. 12, pp. 1244–1256, 2011, doi: 10.1016/j.cemconres.2010.12.001.

[7] Z. Giergiczny, "Fly ash and slag", *Cement and Concrete Research*, vol. 124, art. no. 105826, 2019, doi: 10.1016/j.cemconres.2019.105826.

[8] J. Singh and S.P. Singh, "Development of alkali-activated cementitious material using copper slag", *Construction and Building Materials*, vol. 211, pp. 73–79, 2019, doi: 10.1016/j.conbuildmat.2019.03.233.

[9] J.L. Provis, A. Palomo, and C. Shi, "Advances in understanding alkali-activated materials", *Cement and Concrete Research*, vol. 78, Part A, pp. 110–125, 2015, doi: 10.1016/j.cemconres.2015.04.013.

[10] J.L. Provis, "Alkali-activated materials", *Cement and Concrete Research*, vol. 114, pp. 40–48, 2018, doi: 10.1016/j.cemconres.2017.02.009.

[11] B. Singh, G. Ishwarya, M. Gupta, and S.K. Bhattacharyya, "Geopolymer concrete: A review of some recent developments", *Construction and Building Materials*, vol. 85, pp. 78–90, 2015, doi: 10.1016/j.conbuildmat.2015.03.036.

[12] P. Cong and Y. Cheng, "Advances in geopolymer materials: A comprehensive review", *Journal of Traffic and Transportation Engineering (English Edition)*, vol. 8, no. 3, pp. 283–314, 2021, doi: 10.1016/j.jtte.2021.03.004.

[13] F. Puertas, S. Martínez-Ramírez, S. Alonso, and T. Vázquez, "Alkali-activated fly ash/slag cements: Strength behaviour and hydration products", *Cement and Concrete Research*, vol. 30, no. 10, pp. 1625–1632, 2000, doi: 10.1016/S0008-8846(00)00298-2.

[14] A. Fernández-Jiménez and A. Palomo, "Composition and microstructure of alkali activated fly ash binder: Effect of the activator", *Cement and Concrete Research*, vol. 35, no. 10, pp. 1984–1992, 2005, doi: 10.1016/j.cemconres.2005.03.003.

[15] C.R. Kaze, G.L. Lecomte-Nana, A. Adesina, J.G.D. Nemaleu, E. Kamseu, and U.C. Melo, "Influence of mineralogy and activator type on the rheology behaviour and setting time of laterite based geopolymer paste", *Cement and Concrete Composites*, vol. 126, art. no. 104345, 2022, doi: 10.1016/j.cemconcomp.2021.104345.

[16] I. Harbouz, E. Roziere, A. Yahia, and A. Loukili, "Printability assessment of cement-based materials based on rheology, hydration kinetics, and viscoelastic properties", *Construction and Building Materials*, vol. 325, art. no. 126810, 2022, doi: 10.1016/j.conbuildmat.2022.126810.

[17] G. Peng, J. Wu, K. Huang, C. Shi, X. Hu, and D. Niu, "Research on workability, mechanics, and durability of cementitious grout: A critical review", *Construction and Building Materials*, vol. 449, art. no. 138374, 2024, doi: 10.1016/j.conbuildmat.2024.138374.

[18] M. Palacios, P.F. Banfill, and F. Puertas, "Rheology and setting of alkali-activated slag pastes and mortars: Effect of organic admixture", *ACI Materials Journal*, vol. 105, no. 2, pp. 140–148, 2008, doi: 10.14359/19754.

[19] A. Albar, M. Chougan, M.J. Al-Kheetan, M.R. Swash, and S.H. Ghaffar, "Effective extrusion-based 3D printing system design for cementitious-based materials", *Results in Engineering*, vol. 6, art. no. 100135, 2020, doi: 10.1016/j.rineng.2020.100135.

[20] N. Li, C. Shi, and Z. Zhang, "Understanding the roles of activators towards setting and hardening control of alkali-activated slag cement", *Composites Part B: Engineering*, vol. 171, pp. 34–45, 2019, doi: 10.1016/j.compositesb.2019.04.024.

[21] M. Wang, C. Zhang, P. Jiang, J. Yan, R. Liu, and M. Chen, "Effects of temperature and bleeding on rheology of cement paste", *Construction and Building Materials*, vol. 403, art. no. 133085, 2023, doi: 10.1016/j.conbuildmat.2023.133085.